

Molecular Motion in Ammonium Hydrogendifluoride Studied by Pulsed NMR

Yoshihiro FURUKAWA* and Hideko KIRIYAMA

The Institute of Scientific and Industrial Research, Osaka University, Yamada-ka, Suita, Osaka 565

(Received July 17, 1978)

The proton and fluorine-19 spin-lattice relaxation times, T_1 and $T_{1\rho}$, in polycrystalline ammonium hydrogendifluoride were measured in the temperature range 142—345 K to elucidate the molecular motion of cation and anion. Below 200 K, the relaxation rates of both nuclei can be accounted for by dipolar interactions modulated via the isotropic reorientation of NH_4^+ ions. The $\log T_{1\rho}$ versus $1/T$ curves above 200 K exhibit two distinct minima, suggesting that two crystallographically nonequivalent HF_2^- ions undergo 180° -flips about their two-fold axes with different correlation times. The activation energy of the NH_4^+ reorientation was determined to be 25.5 ± 1.0 kJ/mol from the T_1 data, while those of the 180° -flips were estimated from the $T_{1\rho}$ data to be about 40 and 60 kJ/mol for the two types of anions. These relaxation mechanisms have been confirmed by further experiments on a partially deuterated sample.

A series of alkali-metal hydrogendifluorides have occasioned much interest in the very short, nearly symmetric hydrogen-bond of the $[\text{F}-\text{H}-\text{F}]^-$ ion and in the motional state of such a dumbbell-like anion. The hydrogendifluorides of heavy alkali-metals, such as K, Rb, and Cs, transform to cubic phases at high temperatures because rapid, random reorientations of linear HF_2^- ions give rise to an effectively cubic symmetry.¹⁾ It was also recognized from the previous NMR measurements that the HF_2^- ions are 180° -flipping in the low-temperature phase.^{2,3)} On the other hand, the compounds of light alkali-metals such as Li and Na, and of NH_4^+ , have no phase transitions, suggesting that even if the 180° -flip motion takes place, it persists up to their melting points. The NH_4^+ ion has some freedom of reorientation and a possibility of forming another type of hydrogen bond between $\text{N}(\text{NH}_4^+)$ and $\text{F}(\text{HF}_2^-)$ in addition to the hydrogen bond in an $[\text{F}-\text{H}-\text{F}]^-$ ion just described. It is therefore worthwhile to investigate the ionic motions of nearly spherical NH_4^+ and dumbbell-like HF_2^- ions in NH_4HF_2 crystals and to compare the results obtained with those in potassium hydrogendifluoride.³⁾

The crystal structure of NH_4HF_2 contains four chemical formula units in its orthorhombic cell; the HF_2^- ions are distinguished between two crystallographically nonequivalent $\text{HF}_2^-(1)$ and $\text{HF}_2^-(2)$, whereas the ammonium ions are all equivalent.⁴⁾ The crystal structure can be described as a superstructure of the caesium chloride type, although it is distorted by the presence of rod-shaped HF_2^- ions and by interionic hydrogen bonds.

In this paper, the results of pulsed NMR of both ^1H and ^{19}F nuclei in NH_4HF_2 are reported, and models of the isotropic reorientation of the NH_4^+ ion and the two types of 180° -flipping of the HF_2^- ions are proposed.

Experimental

Powdered NH_4HF_2 was prepared from an aqueous solution of NH_4F and a slight excess of HF acid; it was then recrystallized twice from the aqueous solution. The sample used was identified from its X-ray powder diffraction pattern.⁴⁾

A Bruker B-KR 322s frequency-variable, pulsed NMR spectrometer was employed to determine the magnetic relaxation times, T_1 and $T_{1\rho}$, of ^1H and ^{19}F nuclei. The spin-

lattice relaxation time, T_1 , was measured by use of the 180° - t - 90° pulse sequence at 60 and 20 MHz for ^1H and at 56.442 and 18.814 MHz for ^{19}F nuclei. The relaxation time in the rotating frame, $T_{1\rho}$, was determined by the spin-locking method. The temperature of the sample was controlled to within ± 0.5 K by using an Ohkura EC 61 temperature controller and was measured with a copper-constantan thermocouple calibrated before measurements.

Results

Figure 1 shows the temperature dependences, as a semilogarithmic plot versus inverse temperature, of proton $T_1(\text{H})$ and fluorine-19 $T_1(\text{F})$ obtained at 60 and 56.442 MHz respectively, together with the $T_{1\rho}(\text{H})$ at the r.f. field strength 10 G. The $T_{1\rho}(\text{F})$ could not be measured because of its poor signal, resulting from a very short free-induction-decay (FID). Below about 200 K, the magnetization-recovery curve for the T_1 process of either nucleus became markedly non-exponential, owing to heteronuclear H-F dipole interaction.⁵⁾ The recovery curve was, therefore, resolved into two exponential terms, according to the equation $\langle I_0 - I_z \rangle / 2I_0 = A \exp(-t/T_1') + B \exp(-t/T_1'')$; here I_z and I_0 are the z-components of the I-spin (^1H or ^{19}F) magnetization at time t and at thermal equilibrium, respectively, A and B are constants, and T_1' and T_1'' denote the short and long relaxation times, respectively.³⁾ Above 200 K, although the recovery curve was slightly non-exponential, the T_1 value as well as the $T_{1\rho}$ one was approximated by a single relaxation time, which was defined as the time necessary for the $\langle I_0 - I_z \rangle / 2I_0$ to fall to $1/e$ of its initial value. The frequency dependence of the T_1 value was examined by additional measurements at 20 MHz for ^1H and 18.814 MHz for ^{19}F nuclei; these plots were omitted from Fig. 1 for simplicity.

The $\log T_1(\text{H})$ vs. $1/T$ curve at 60 MHz exhibits a deep T_1 minimum at $\text{kK}/T \approx 4.4$; the corresponding $T_{1\rho}$ minimum occurs at $\text{kK}/T \approx 6.6$. Two additional $T_{1\rho}$ minima are recognized at $\text{kK}/T \approx 3.0$ and 4.0, indicating that the molecular motions of NH_4^+ and/or HF_2^- ions are rather complex within the crystal lattice.

In order to uncover further details of the ionic motion in the high-temperature region, the measurements of the $T_1(\text{F})$ and $T_{1\rho}(\text{F})$ were extended to a sample of partially deuterated NH_4HF_2 . The results are shown as

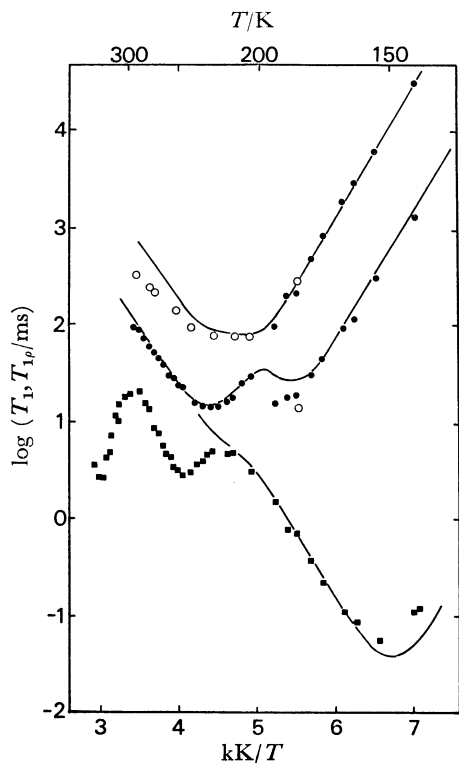


Fig. 1. Temperature dependences of spin-lattice relaxation times in NH_4HF_2 : (●) $T_1(\text{H})$ at 60 MHz, (○) $T_1(\text{F})$ at 56.442 MHz, and (■) $T_{1\rho}(\text{H})$ at 10 G. The solid lines indicate the calculated temperature dependences of T_1 and $T_{1\rho}(\text{H})$ for randomly reorienting NH_4^+ ions.

experimental points in Fig. 2. The deuterium content was estimated to be about 65% from the ratio of the $T_1(\text{F})$ minimum value for the nondeuterated sample to that for the partially deuterated one; these minima will be assigned to the NH_4^+ isotropic reorientation later.

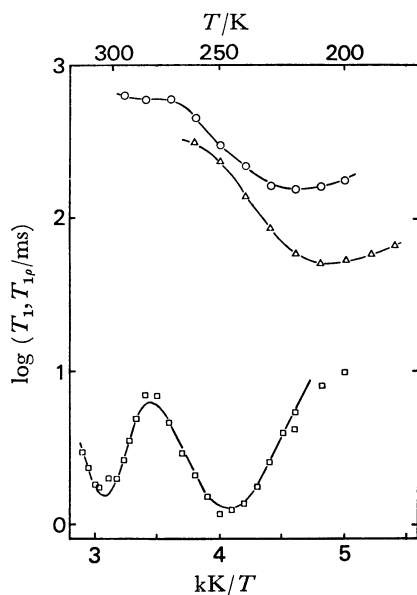


Fig. 2. Temperature dependences of spin-lattice relaxation times in 65% $d\text{-NH}_4\text{HF}_2$: (○) $T_1(\text{F})$ at 56.442 MHz, (△) $T_1(\text{F})$ at 18.814 MHz, and (□) $T_{1\rho}(\text{F})$ at 6.5 G. The lines are drawn to guide the eye.

Isotropic Reorientation of NH_4^+ Ions. The relaxation process for T_1 below room temperature is ascribable to NH_4^+ isotropic reorientation, because such a short $T_1(\text{H})$ minimum as 14 ms is characteristic of NH_4^+ reorientation. In this case, the ^1H relaxation rate is governed mainly by the intraionic H–H dipolar interaction and partially by the interionic dipolar interactions, $\text{H}(\text{NH}_4^+) \text{--} \text{H}(\text{NH}_4^+)$ and $\text{H}(\text{NH}_4^+) \text{--} \text{H}(\text{HF}_2^-)$, and the heteronuclear $\text{H}(\text{NH}_4^+) \text{--} \text{F}(\text{HF}_2^-)$ one. Among these, the contribution of the homonuclear H–H interaction to the ^1H relaxation rate is expressed as follows:

$$T_1(\text{HH})^{-1} = (2/3)\gamma_{\text{H}}^2 \Delta M_{\text{HH}} f(\omega_{\text{H}}, \tau_{\text{H}}), \quad (1a)$$

$$f(\omega, \tau) = \tau / (1 + \omega^2 \tau^2) + 4\tau / (1 + 4\omega^2 \tau^2). \quad (1b)$$

The quantity ΔM_{HH} is the reduction in the second moment of the ^1H absorption spectrum due to the H–H dipolar interaction associated with the NH_4^+ reorientation; τ_{H} stands for the correlation time for the NH_4^+ motion; the other symbols have their usual meaning.

On the other hand, the relaxation due to heteronuclear dipole interaction between ^1H and ^{19}F nuclei can be expressed by the following pair of coupled equations:⁵⁾

$$d\langle I_z \rangle / dt = -\langle I_z - I_0 \rangle / T_1(\text{IS}) - \langle S_z - S_0 \rangle / T_1'(\text{IS}), \quad (2a)$$

$$d\langle S_z \rangle / dt = -\langle I_z - I_0 \rangle / T_1'(\text{SI}) - \langle S_z - S_0 \rangle / T_1(\text{SI}), \quad (2b)$$

where I and S stand for H and F, respectively. Each relaxation time in Eq. 2 can be calculated in the same manner as with $(\text{NH}_4)_2\text{BeF}_4$.⁵⁾ Thus,

$$T_1(\text{FH})^{-1} = (3/16)\gamma_{\text{F}}^2 \Delta M_{\text{FH}} g(\omega_{\text{F}}, \omega_{\text{H}}, \tau_{\text{H}}), \quad (3a)$$

$$T_1'(\text{FH})^{-1} = (3/16)\gamma_{\text{F}}^2 \Delta M_{\text{FH}} g'(\omega_{\text{F}}, \omega_{\text{H}}, \tau_{\text{H}}), \quad (3b)$$

$$g(\omega_{\text{I}}, \omega_{\text{S}}, \tau) = \tau / [1 + (\omega_{\text{I}} - \omega_{\text{S}})^2 \tau^2] + 3\tau / (1 + \omega_{\text{I}}^2 \tau^2) + 6\tau / [1 + (\omega_{\text{I}} + \omega_{\text{S}})^2 \tau^2], \quad (3c)$$

$$g'(\omega_{\text{I}}, \omega_{\text{S}}, \tau) = -\tau / [1 + (\omega_{\text{I}} - \omega_{\text{S}})^2 \tau^2] + 6\tau / [1 + (\omega_{\text{I}} + \omega_{\text{S}})^2 \tau^2]. \quad (3d)$$

The ΔM_{FH} is again the reduction in the ^{19}F second moment due to the F–H dipolar interaction *via* the NH_4^+ reorientation. By taking into account the abundances of ^1H and ^{19}F nuclei in the crystal,⁵⁾ the ^1H relaxation rates due to the heteronuclear H–F interaction, $T_1(\text{HF})^{-1}$ and $T_1'(\text{HF})^{-1}$, can be easily related to Eq. 3. The $T_1(\text{FF})^{-1}$ of course, need not be considered because the F–F dipole interaction is not modulated *via* the NH_4^+ reorientation. The observed relaxation rates are given by the eigenvalues of the relaxation matrix:

$$\begin{pmatrix} T_1(\text{HH})^{-1} + T_1(\text{HF})^{-1} & T_1'(\text{HF})^{-1} \\ T_1'(\text{FH})^{-1} & T_1(\text{FH})^{-1} \end{pmatrix}.$$

The ΔM_{HH} value was first evaluated from the atomic positions as determined by X-rays.⁴⁾ It was too large to explain the observed $T_1(\text{H})$ minimum, because of the rather short N–H distance (0.88 Å) used. So the values of ΔM_{HH} and ΔM_{FH} were recalculated by taking the $r(\text{N–H})$ distance as 1.059 Å (corresponding to 1.73 Å for the $r(\text{H} \cdots \text{H})$ distance in a tetrahedral NH_4^+ ion)⁶⁾ and the two nonequivalent $r(\text{F–F})$ distances as 2.297 and 2.291 Å in both hydrogen-centered $[\text{F–H–F}]^-$ ions.⁷⁾ For the rigid lattice model, the theoretical second moments thus obtained are $M_{\text{HH}} = 41.80$, $M_{\text{HF}} = 30.01$ G² for ^1H and $M_{\text{FF}} = 4.18$, $M_{\text{FH}} = 84.97$ G² for ^{19}F nuclei. On the other hand, a model of the NH_4^+

isotropic reorientation yields $M_{\text{HH}}=5.55$, $M_{\text{HF}}=26.56$, $M_{\text{FF}}=4.18$, and $M_{\text{FH}}=75.20$ G². By substituting the calculated second moments into Eqs. 1 and 3 and by diagonalizing the relaxation matrix, one can calculate the following T_1 minimum values for the two nuclei: $T_1(\text{H})_{\text{min}}=14.3$ and $T_1(\text{F})_{\text{min}}=79.5$ ms. The experimental values to be compared with these T_1 minima were 13.5 and 73 ms, respectively. The good agreement between the calculated and experimental values indicates that the NH_4^+ isotropic reorientation is responsible for the relaxation process in this temperature region. The activation energy, E_a , of the NH_4^+ reorientation was determined to be 25.5 ± 1.0 kJ/mol from the slope of the $\log T_1'$ (or T_1'') vs. $1/T$ line on its low-temperature side, by assuming that $\tau=\tau_0 \exp(E_a/RT)$. The solid lines for $T_1(\text{H})$ and $T_1(\text{F})$ in Fig. 1 were calculated from Eqs. 1 and 3 with the relaxational parameters, τ_0 and E_a , listed in Table 1.

TABLE 1. RELAXATIONAL PARAMETERS IN NH_4HF_2

	$E_a/\text{kJ mol}^{-1}$	τ_0/s	Motion
NH_4^+	25.5 ± 1.0	2.5×10^{-15}	isotropic
$\text{HF}_2^-(1)$	≈ 60	$\approx 10^{-15}$	180°-flip
$\text{HF}_2^-(2)$	≈ 40	$\approx 10^{-14}$	180°-flip
HF_2^- in KHF_2^a	50.5	6.4×10^{-15}	180°-flip

a) Ref. 3.

In the weak collision limit, $T_{1\rho}(\text{H})$ is given by the equation corresponding to Eqs. 1 and 3 for $T_1(\text{HH})$, etc.⁵⁾

$$T_{1\rho}(\text{H})^{-1} = (1/3)\gamma_{\text{H}}^2 \Delta M_{\text{HH}} f_{\rho}(\omega_{\text{H}}, \tau_{\text{H}}) + (3/32)\gamma_{\text{H}}^2 \Delta M_{\text{HF}} g_{\rho}(\omega_{\text{H}}, \omega_{\text{F}}, \tau_{\text{H}}), \quad (4a)$$

$$f_{\rho}(\omega_1, \tau) = 3\tau/(1+4\omega_1^2\tau^2) + 5\tau/(1+\omega_1^2\tau^2) + 2\tau/(1+4\omega_1^2\tau^2), \quad (4b)$$

$$g_{\rho}(\omega_1, \omega_8, \tau) = 4\tau/(1+\omega_1^2\tau^2) + \tau/[1+(\omega_1-\omega_8)^2\tau^2] + 9\tau/(1+\omega_1^2\tau^2) + 6\tau/[1+(\omega_1+\omega_8)^2\tau^2]. \quad (4c)$$

Although our experimental condition ($H_1=\omega_1/\gamma_{\text{H}}=10$ G) wasn't sufficient for the weak collision limit, we tried to approximate the problem by this limit. Thus, the theoretical $\log T_{1\rho}(\text{H})$ vs. $1/T$ curve was calculated from Eq. 4 with the same relaxational parameters as those in the T_1 calculation. As compared in Fig. 1, the overall agreement between the calculation and the observation is good, except for the temperature range above 200 K.

180°-Flipping of HF_2^- Ions. The relaxational behavior above 200 K is rather complicated. The $T_{1\rho}$ data in Figs. 1 and 2 clearly suggest the presence of other relaxational processes. The FID signals of both nuclei show no lengthening due to self-diffusion of the NH_4^+ or HF_2^- ions, even at the highest temperature of measurement (345 K). Hence, the 180°-flip motion of the HF_2^- ion becomes of much interest, because it can contribute to the relaxation rates of both nuclei in the high temperature region, as evidenced in the low-temperature phase of potassium hydrogendifluoride.^{2,3)}

If that is the case, at temperatures higher than 200 K the $T_{1\rho}(\text{H})$ in NH_4HF_2 may be governed by the H-F dipolar interaction modulated via the 180°-flips of the HF_2^- ions. The two crystallographically nonequivalent

HF_2^- ions may have different correlation times, τ_1 , and τ_2 , for their individual 180°-flips. If these correlation times are greatly different from each other, then the two corresponding $T_{1\rho}$ minima would be well separated, as can be seen in Fig. 1. The ^1H relaxation rate due to the H-F dipolar interaction via the 180°-flip is given in a spatial average form as follows:³⁾

$$T_{1\rho}(\text{HF})^{-1} = \gamma_{\text{H}}^2 \gamma_{\text{F}}^2 \hbar^2 / 80 \sum_{\beta} [r_{\text{HF}}(\beta)^{-6} + r_{\text{HF}}(\delta)^{-6} - r_{\text{HF}}(\beta)^{-3} r_{\text{HF}}(\delta)^{-3} (3 \cos^2 \Delta_{\beta\delta} - 1)] g_{\rho}(\omega_{\text{H}}, \omega_{\text{F}}, \tau_i), \quad (5)$$

where τ_i stands for τ_1 and τ_2 , β and δ denote two positions of a given F atom, $r_{\text{HF}}(\beta)$ is the distance between the hydrogen and the fluorine atom at a β -site, and $\Delta_{\beta\delta}$ is the angle between two H-F internuclear vectors. In the actual calculation based on Eq. 5, four hydrogen atoms of a rapidly rotating NH_4^+ ion were located at the center of the ion, in the usual manner.

On the other hand, the $T_{1\rho}(\text{F})$ in the 65% $d\text{-NH}_4\text{HF}_2$ may be governed by the homonuclear F-F dipolar interaction. The relaxation rate due to 180°-flipping of water molecules has been derived by Look and Lowe.⁸⁾ In order to apply the Look and Lowe equation to the present case, the equation was modified to hold for two independent correlation times. The results are presented only in the $T_{1\rho}^{-1}$ form for a single crystal:

$$T_{1\rho}(\text{FF})^{-1} = 3\gamma_{\text{F}}^4 \hbar^2 I_{\text{F}}(I_{\text{F}}+1)/64N \sum_{i \neq j} [\zeta^{(0)} J(2\omega_{1\text{F}}, \tau_i) + 10\zeta^{(1)} J(\omega_{\text{F}}, \tau_i) + \zeta^{(2)} J(2\omega_{\text{F}}, \tau_i) + \xi^{(0)} J(2\omega_{1\text{F}}, \tau_j) + 10\xi^{(1)} J(\omega_{\text{F}}, \tau_j) + \xi^{(2)} J(2\omega_{\text{F}}, \tau_j) + \eta^{(0)} J(2\omega_{1\text{F}}, \tau_{ij}) + 10\eta^{(1)} J(\omega_{\text{F}}, \tau_{ij}) + \eta^{(2)} J(2\omega_{\text{F}}, \tau_{ij})], \quad (6a)$$

$$\zeta^{(q)} = |\chi_{ij}^{(q)}(\beta_i, \beta_j) + \chi_{ij}^{(q)}(\beta_i, \delta_j) - \chi_{ij}^{(q)}(\delta_i, \beta_j) - \chi_{ij}^{(q)}(\delta_i, \delta_j)|^2, \quad (6b)$$

$$\xi^{(q)} = |\chi_{ij}^{(q)}(\beta_i, \beta_j) - \chi_{ij}^{(q)}(\beta_i, \delta_j) + \chi_{ij}^{(q)}(\delta_i, \beta_j) - \chi_{ij}^{(q)}(\delta_i, \delta_j)|^2, \quad (6c)$$

$$\eta^{(q)} = |\chi_{ij}^{(q)}(\beta_i, \beta_j) - \chi_{ij}^{(q)}(\beta_i, \delta_j) - \chi_{ij}^{(q)}(\delta_i, \beta_j) + \chi_{ij}^{(q)}(\delta_i, \delta_j)|^2, \quad (6d)$$

$$\tau_{ij}^{-1} = \tau_i^{-1} + \tau_j^{-1}, \quad (6e)$$

$$J(\omega, \tau) = \tau/(1+\omega^2\tau^2), \quad (6f)$$

where $\chi_{ij}^{(q)}$ ($q=0, 1$, and 2) is the usual orientation function.⁸⁾ When $\tau_i=\tau_j$, of course, Eq. 6 is identical with the Look and Lowe equation. As a powdered sample was used in this study, Eq. 6 was spatially averaged before use.⁹⁾

In addition, the interionic F-H dipolar interaction also contributes to $T_{1\rho}(\text{F})$. This contribution can be estimated from Eq. 5, taking into account the extent of the deuteration. The contribution from ^2H nuclei was neglected because γ_{F} is very large compared with γ_{D} .

The summations in Eqs. 5 and 6 were carried out up to six or eight neighboring ions around a central $\text{HF}_2^-(1)$ or $\text{HF}_2^-(2)$ ion, respectively. By using the parameters thus obtained, and Eqs. 5 and 6 for $T_{1\rho}$'s, the minimum values of $T_{1\rho}$ were evaluated. In this calculation, the correlation time for the 180°-flip of the $\text{HF}_2^-(2)$ ions was assumed to be shorter than that of the $\text{HF}_2^-(1)$ ions, for a reason to be described later. These values

TABLE 2. CALCULATED AND EXPERIMENTAL VALUES OF $T_{1\rho}$ MINIMA DUE TO THE 180° -FLIPS OF THE HF_2^- IONS

$T_{1\rho}(\text{H})$ was measured at 10 G in NH_4HF_2 and $T_{1\rho}(\text{F})$ was at 6.5 G in the 65% *d*- NH_4HF_2 .

	$T_{1\rho}(\text{H})_{\text{min}}/\text{ms}$		$T_{1\rho}(\text{F})_{\text{min}}/\text{ms}$	
	Calcd	Exptl	Calcd	Exptl
$\text{HF}_2^-(1)$	2.4	2.2	1.2	1.7
$\text{HF}_2^-(2)$	2.5	1.9	1.1	1.2

are compared with the experimental ones in Table 2. The agreement is fairly good, supporting the idea that the 180° -flip motions of the nonequivalent, linear HF_2^- ions are separately excited at high temperatures. The values of E_a and the pre-exponential factor τ_0 were roughly estimated in a conventional way; these results are included in Table 1 together with those for the NH_4^+ ions.

Discussion

The T_1 observed at all temperatures and the $T_{1\rho}$ in the low-temperature region were well explained by the random reorientation of the NH_4^+ ion, rather than by its C_2 reorientation predicted from the site symmetry (2) of the ammonium nitrogen. An activation energy E_a of 25.5 kJ/mol in the present NH_4HF_2 suggests that the hydrogen-bonds between $\text{N}(\text{NH}_4^+)$ and $\text{F}(\text{HF}_2^-)$ atoms are rather strong, as was anticipated from the short N—F distances (2.797 Å twice and 2.822 Å twice)⁴⁾ and also from the highly ionic charge on the F atom ($-0.83e$).¹⁰⁾ The values of E_a and the N(H)···F distance in NH_4HF_2 are intermediate between those found in NH_4F (42 kJ/mol, 2.71 Å)¹¹⁾ and NH_4BF_4 (6.3 kJ/mol, 2.92 Å);¹²⁾ an E_a value of 3–5 kJ/mol in NH_4PF_6 is the lowest one,¹³⁾ but the N···F distance (2.4 Å) seems to be too small to compare with the above three, possibly owing to the highly disordered structure.¹⁴⁾ These comparisons indicate that the activation energy for the NH_4^+ reorientation strongly depends on the $\text{NH}\cdots\text{F}$ hydrogen-bond distance as well as on the dimensions of a combined anion.

On the other hand, the $T_{1\rho}$ data above 200 K could be interpreted in terms of the stepwise 180° -flip motions

of the two nonequivalent HF_2^- ions. According to the X-ray results, the intraion F—(H)—F bond distances in both HF_2^- ions are nearly the same within the experimental errors, whereas the interionic hydrogen-bond distances $\text{F}\cdots(\text{H})\text{N}$ significantly differ from each other (2.797 for $\text{HF}_2^-(1)$ and 2.822 Å for $\text{HF}_2^-(2)$ ions).⁴⁾ It was therefore expected that the latter $\text{HF}_2^-(2)$ ion would be more mobile and be characterized by a lower activation energy, *i.e.* a shorter correlation time. The preceding analysis of the $T_{1\rho}$ data based on this assumption yielded approximate E_a values of 60 for $\text{HF}_2^-(1)$ and 40 kJ/mol for $\text{HF}_2^-(2)$, both of which are roughly comparable to the 50 kJ/mol obtained in KHF_2 (Table 1).³⁾ However, the difference of E_a in the ammonium salt seems to be too large to arise from the difference in the hydrogen-bond strength alone. This finding leads us to point out that the different HF_2^- ions take different pathways of flipping. For an isolated molecular ion, the two-fold (C_2) axis of flip cannot be defined uniquely on the molecular mirror plane, because the symmetry of the ion is ∞/m ($\text{D}_{\infty h}$). Furthermore, the X-ray results, especially the strongly anisotropic temperature factors, provided valuable information on the ionic motion. That is, the maximum amplitude of either fluorine atom due to ionic libration is observed perpendicular to the mean plane of the three hydrogen-bonds, one of which is intraionic and the other two interionic.⁴⁾ As can be seen in Fig. 3, both types of HF_2^- ions locate at the sites of the same symmetry 2/m, but the ionic axis of $\text{HF}_2^-(1)$ is perpendicular to the mirror plane (100), while the axis of $\text{HF}_2^-(2)$ ion lies on this mirror plane. Under these circumstances, the $\text{HF}_2^-(2)$ ion may rotate about the ionic and crystallographic C_2 axis, *i.e.* on the plane (100), without destroying any initial site symmetry. In contrast to this, the flipping pathway of the $\text{HF}_2^-(1)$ ion about the C_2 -axis, which lies on the hydrogen-bonded plane, does break down the site symmetry and then the motion is highly hindered by the repulsion from the neighboring fluorine atoms, when the linear anion goes across the crystal mirror plane. Although this explanation is only a simple and tentative one, it seems likely that such a steric hindrance contributes to the difference in the activation energies.

The authors are grateful to Professor Emeritus Ryôiti Kiriya for his continued interest and encouragement. This work was partly supported by a Grant-in-Aid for Scientific Research from the Ministry of Education (No. 047076).

References

- 1) R. Kruh, K. Fuwa, and T. E. McEver, *J. Am. Chem. Soc.*, **78**, 4256 (1956).
- 2) Yu. G. Kriger, S. P. Gabuda, and N. K. Moroz, *Fiz. Tverd. Tela (Leningrad)*, **17**, 3420 (1975) [*Sov. Phys. Solid State*, **17**, 2239 (1976)]; Yu. G. Kriger, N. K. Moroz, and S. P. Gabuda, *ibid.*, **18**, 891 (1975) [*ibid.*, **18**, 514 (1976)].
- 3) Y. Furukawa and H. Kiriya, *Bull. Chem. Soc. Jpn.*, **51**, 3438 (1978).
- 4) T. R. R. McDonald, *Acta Crystallogr.*, **13**, 113 (1960).
- 5) D. E. O'Reilly, E. M. Peterson, and T. Tsang, *Phys.*

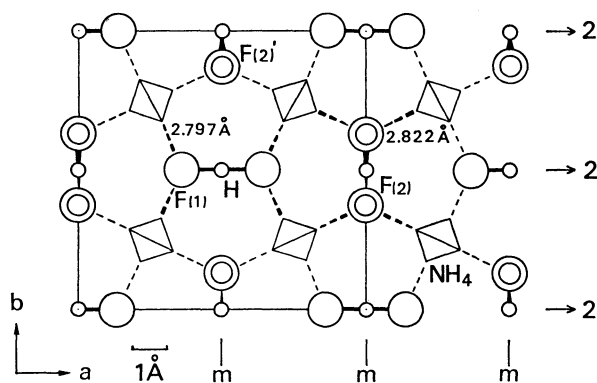


Fig. 3. The crystal structure of NH_4HF_2 projected along the c axis after McDonald.⁴⁾

Rev., **160**, 333 (1967).

6) D. E. O'Reilly and T. Tsang, *J. Chem. Phys.*, **46**, 1291 (1967).

7) H. L. Carrell and J. Donohue, *Israel J. Chem.*, **10**, 195 (1972).

8) D. C. Look and I. J. Lowe, *J. Chem. Phys.*, **44**, 2995 (1966).

9) K. Sagisawa, H. Kiriyaama, and R. Kiriyaama, *Bull. Chem. Soc. Jpn.*, **51**, 1942 (1978).

10) P. Van Hecke, H. W. Spiess, and U. Haeberlen, *J. Magn. Reson.*, **22**, 103 (1976).

11) L. E. Drain, *Discuss. Faraday Soc.*, **19**, 200 (1955).

12) J. J. Van Rensburg and J. C. A. Boeyens, *J. Solid State Chem.*, **5**, 79 (1972).

13) L. Niemela and J. Tuohi, *Ann. Univ. Turku, Ser. A*, **1**, 12 (1970).

14) R. W. G. Wyckoff, "Crystal Structures," 2nd ed, Interscience Publishers, New York (1965), Vol. 3, p. 326.
